Journal of Advances in Science, Engineering and Technology

Zinc Sulphide Nanoparticles as a Viable Alternative to Platinum Counter Electrode for Low-Cost Dye Sensitized Solar Cells

Vincent Bungei, Tabitha Amollo*, Duke Oeba

Department of Physics, Egerton University, Faculty of Science, P.O Box 536-20115, Egerton, Nakuru, Kenya.

ABSTRACT

Dye-sensitized solar cell (DSSC) is considered one of the most promising and economical emerging solar energy conversion technologies because of its low production cost and potential efficiencies. However, an expensive and scarce platinum (Pt) is used in their counter electrode (CE). Additionally, Pt CE corrodes as a result of the oxidized electrolyte's chemical attack and requires high manufacturing temperatures. This makes the production of DSSC relatively expensive. This research focused on preparing and utilizing zinc sulphide (ZnS) nanoparticles as the CE in DSSC. The nanoparticles were synthesized using the low-cost chemical reduction method. The X-Ray diffraction (XRD) measurement showed high crystallinity of the nanocomposite. The Fourier Transform Infrared (FTIR) measurements showed the presence of Zn-S bond stretching vibrations. As compared to Pt-based CE, ZnS-based CE demonstrated slightly lower conductivity of 54.41 S/m to 379.85 S/m for Pt. Power conversion efficiency (PCE) was noted to improve from 0.07% for unannealed ZnS-based CE to 1.1 % for ZnS-based CE annealed at 400 ^{0}C. The improvement is associated with enhanced crystalline quality of ZnS nanoparticles upon annealing the CE at 400 ^{0}C. Therefore, ZnS nanoparticles show great promise as a cost-effective alternative counter electrode for DSSC with further material properties optimization.

ARTICLE INFO

Keywords:
Chemical reduction,
Electrical conductivity,
Metallic nanoparticles,
Photovoltaic parameters.

Article History:
Received 6 November 2025
Received in revised form 18 November 2025
Accepted 27 November 2025
Available online 17 February 2026

1. Introduction

Dye-sensitized solar cells (DSSCs) present an appealing pathway toward low-cost, flexible, and lightweight photovoltaic systems (Kharboot et al., 2023). Their current success of a PCE of about 15.2 % (Ibrayeva et al., 2025) hinges not only on efficient light harvesting at the photoanode but equally on the performance of the counter electrode (CE), which catalyzes the reduction of the redox electrolyte and enables charge circulation. Historically, platinum (Pt) has been the material of choice for the CE in DSSCs due to its excellent catalytic activity and electrical conductivity (Ding et al., 2023). DSSC has also been reported to have improved in stability, with the most current maintaining about 75% of its power conversion efficiency (PCE) after 1400 hours while operating at approximately 23°C (Ibrayeva et al., 2025).

However, the high cost, scarcity, and complex fabrication requirements of Pt pose significant barriers for large-scale commercialization (Dhonde et al., 2022). As a result, researchers have turned to earth-abundant, low-cost materials that can deliver comparable electrocatalytic and conductive performance.

The first natural semiconductor discovered was zinc sulphide (ZnS), exhibiting a band gap of 3.7 eV in the cubic zinc blende and 3.76 eV in the hexagonal wurtzite (Fang et al., 2010). It is a low-cost, non-toxic semiconductor with interesting optoelectronic properties (Choudapur et al., 2019). ZnS offers chemical stability, abundant availability, and tunable nanostructure, making it attractive for DSSC applications (Lihua et al., 2018). In bulk form, ZnS suffers from poor electrical conductivity and limited catalytic activity toward the triiodide/iodide (I_3^-/I^-) redox couple. However, recent investigations show that when properly engineered, ZnS nanostructures can significantly improve charge transfer kinetics and device performance (Li et al., 2015). Sulfur (S) content has a substantial impact on the morphological, optical, and electrical properties of ZnS because it directly influences the material's stoichiometry, defect density, and crystal structure (Choudapur et al., 2019). For instance, if the ideal ratio between Zn and S is deviated, S vacancies can

* Corresponding author. e-mail: tamollo@egerton.ac.ke
Editor: Victor Odari, Masinde Muliro University of Science and Technology, Kenya.
Citation: Bungei V., Amollo T., & Oeba D. (2026). Zinc Sulphide Nanoparticles as a Viable Alternative to Platinum Counter Electrode for Low-Cost Dye Sensitized Solar Cells. Journal of Advances in Science, Engineering and Technology 3(1), 1 – 6.

form within the lattice. This affects the nucleation and growth kinetics and leads to notable variations in particle size, surface morphology, and crystallinity (Jubeer et al., 2023). Therefore, ZnS nanoparticles are one of the most effective nanoparticles of choice for enhanced DSSCs (Kim et al., 2017). This is because ZnS is a direct band gap material with good chemical durability against oxidation and hydrolysis (Naeimi et al., 2014). Additionally, ZnS is abundant in nature (Kang et al., 2018). Despite notable progress in improving the efficiency of DSSCs, the widespread applications of these devices remain constrained by the high cost, scarcity, and complex fabrication requirements of Pt. This has made their large-scale commercialization unachievable. Although several alternative materials, such as carbon-based materials, conducting polymers, and traditional metal sulphides, have been explored, studies focusing specifically on the catalytic and electrochemical performances of pure ZnS nanoparticles as a substitute for Pt are still limited. Furthermore, the influence of the synthesis route and structural properties of ZnS on the overall photovoltaic performance of DSSCs has not been fully elucidated. Therefore, this study endeavored to bridge this knowledge gap by investigating ZnS nanoparticles as a viable, low-cost alternative to Pt for CE applications in DSSCs. Herein this research presents the synthesis of ZnS nanoparticles through the chemical reduction method, and the utilization of the nanomaterial as the CE in fabricating DSSCs. We characterized the structural properties of the nanomaterial and benchmarked the photovoltaic performance of DSSCs employing pure ZnS CEs against standard platinum CEs.

2. Material and Methodology

2.1. Materials Acquisition, Substrate cleaning, Synthesis and Characterization of Nanomaterials.

Ethylene glycol (EG), thiourea (99.9%), zinc chloride (98 %), acid were all purchased from Kobian Kenya, but the products were from Sigma Aldrich. Titanium (IV) oxide (99.5%), hexa-chloroplatinic acid (H_2PtCl_6), Triton X-114, PROTEIN GRADE® Detergent, 10% Solution, Sterile-Filtered, lithium iodide (99.9 %), iodine (99.999 %), 4-tert-butylpyridine (TBP) (98%), 4-butyl-3-methylimidazolium iodide (BMII) (99.9%), and N-719 dye were acquired from Sigma Aldrich UK-based companies. These were of analytical grade. Indium-doped tin oxide (ITO) substrates of sheet resistance 20 Ωsq^{-1} and dimensions 20 mm x 15 mm and 1.1 mm thickness were purchased from Ossila Ltd.

The substrates were cleaned by first ultrasonicating in a solution containing distilled water and detergent for 10 minutes. The substrates were then rinsed with deionized water to get rid of the detergent before ultrasonicating them for 10 minutes in distilled water. After that, it underwent another ultrasonication for ten minutes in acetone, followed by another ten minutes in isopropanol solution. Finally, the substrates were dried in a vacuum oven for twenty minutes.

To synthesize ZnS, two setups of solutions were made; first, 0.41 mmol of thiourea was slowly introduced into 100 mL of ethylene glycol (EG) for dispersion under continuous magnetic stirring, and the mixture was maintained at 100°C. Separately, 0.41 mmol of anhydrous $ZnCl_2$ was dissolved in 50 mL of EG and heated to 100 °C. The thiourea suspension was then immediately combined with the $ZnCl_2$ solution, and the resulting mixture was further heated to 150 °C to complete the synthesis. After maintaining this temperature for 4 hours, a white suspension was formed, indicating successful synthesis. The resulting suspension was collected via centrifugation, then thoroughly washed with ethanol and double-distilled water to a neutral pH to eliminate impurities. The product was subsequently dried in a vacuum oven at 60 °C for 24 hours.

The resultant ZnS nanoparticles microstructure was determined using a Bruker 800 234 - X-Ray powder diffractometer (9729) CRO tube with 1.54184 Å detector hyroxeye (ID made), while the infrared (IR) spectrum was obtained from a FTIR spectrometer (JASCO 4700) with ATR PRO ONE head and a TGS detector covering a spectral range of 500 to 4000 cm^{-1}, with a resolution of 4.0 cm^{-1} to ensure detailed spectral features. The crystallite size is given by Eq. 1 (Bokuniaeva & Vorokh, 2019).

$$D = \frac{k\lambda}{\beta \cos\theta} \quad (1)$$

Where D is the nanoparticle crystalline size, K represents the Scherrer constant (0.98), λ denotes the wavelength (1.54184), and ß denotes the full width at half maximum (FWHM) (1.3922). A four-point probe (SRM-232-1000, Guardian Manufacturing) was used to measure the sheet resistance of the fabricated counter electrodes.

2.2. Device Fabrication and Characterization

To fabricate the PA of this DSSC, an 8 ml mixture of de-ionized water and ethanol (1:1) was poured into a 100 ml beaker, then 0.4 ml of Triton X-114 and 0.2 ml of acetylacetone were added to the solution and stirred using a magnetic stirrer. 1.0 g of TiO_2 powder was then added to the solution and left to continue stirring for thirty minutes to obtain a homogeneous paste. The diluted paste was then deposited on a precleaned ITO substrate by the spin coating process at 1000 rpm for 60 s. This was then dried at 100 ºC in a vacuum oven and finally annealed at 450 ºC on a hotplate under argon gas for 30 minutes. After annealing, the fabricated PA films were submerged in an ethanol solution containing 0.3 mM N719 for 24 hours to adsorb the dye at room temperature. After removing the dye-adsorbed photoanode from the solution, it was instantly cleaned with ethanol.

The CE was prepared by spin coating ZnS in ethanol solution on the precleaned ITO glass substrate. The spin-coated ZnS film was heated at annealing temperatures of 400ºC for 15 minutes. Fig. 1 shows the side view of the DSSC fabricated with ZnS as the CE. To compare the performance of the ZnS CE, a Pt CE was also prepared by the spin coating technique for reference DSSC. A drop of

hexa-chloroplatinic acid (H_2PtCl_6) solution was spread on the ITO glass substrate and kept for air drying. Then the air-dried film was heat-treated at 400 ºC for 15 minutes to obtain Pt-coated ITO CE. The prepared PA and CE were placed together and clamped firmly. The electrolyte used in our investigation was a combination of 0.5 moles of lithium iodide (LiI), 0.05 moles of iodine (I_2), 0.5 moles of 4-tert-butylpyridine (TBP) additive and 0.6 moles of 4-butyl-3-methylimidazolium iodide (BMII) ionic liquid as demonstrated in Eq. 2 in a solution of acetonitrile and Valero nitrile in the ratio (1:1) (Iranmanesh et al., 2015).

$$0.5\,M\,Li + 0.05\,M\,I_2 + 0.5\,M\,TBP + 0.6\,M\,BMII \quad (2)$$

This electrolyte was applied dropwise between the PA and CE until it wets the entire contact area.

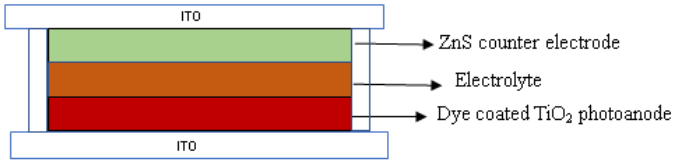

Fig. 1: Cross-sectional view of the fabricated DSSC featuring a TiO_2 photoanode and a ZnS counter electrode.

3. Results and Discussion

3.1. Nanomaterial characterization

3.1.1. Structural properties

The microstructure of the ZnS was investigated by X-ray diffraction. Fig. 2 shows the XRD pattern of the nanomaterial. A cursory check on the diffraction pattern shows that ZnS exhibited four prominent peaks. Three strong diffraction peaks appeared at 2θ values of 28.97º, 48.33º, and 56.82º. The peaks originate from the cubic zinc-blende phase of ZnS in the (111), (202), and (311) planes, respectively. These spectra matched well with JCPDS data (Card No. 05-0566) (Ahmad et al., 2011). Using the Debye-Scherer formula as shown in equation (1), the particle size was determined to be 1.121, 1.190, and 1.234 nm for the 2θ values of 28.97º, 48.33º, and 56.82º, respectively. These small sizes indicate the formation of a nanocrystalline ZnS nanoparticle with a strong quantum confinement effect. These nano-sized particles have a large surface area to volume ratio, which can enhance the catalytic and interfacial properties of the CE (PAWAR, 2013). This, in turn, improves the charge transfer and the overall performance of the cell.

3.1.2. The spectroscopic analysis of functional groups of ZnS nanoparticles

Fig. 3 represents the Fourier Transform Infrared (FTIR) spectra of the synthesized ZnS nanomaterials. The measurements were conducted using 40 scans per second, covering a spectral range of 500 to 4000 cm^{-1}, with a resolution of 4.0 cm^{-1} to ensure detailed spectral features. It gives the characteristic vibrational and / functional groups. The absorption bands at 3667 and 3323 cm^{-1} are typically attributed to the O - H stretching vibration. The bands at 2973 and 2884 cm^{-1} were assigned to C - H stretching. The presence of these peaks implies surface adsorption of water and/or organic residue when under preparation or storage. The absorption bands at 1666 cm^{-1} can be ascribed to H-O-H bending due to the presence of water in the system and without organics (Iranmanesh et al., 2015). On the other hand, bands at 1384 and 1260 cm^{-1} could indicate carbonyl C=O and C-O groups. Metal-oxygen bonds or sulfate vibration were related to the peaks at 1080 and 1046 cm-1. Additionally, distinct absorption bands at around 600 - 900 cm^{-1} were observed. These are assigned to the stretching signatures of Zn-S bonds, confirming the successful formation of ZnS nanoparticles (Aziz et al., 2020).

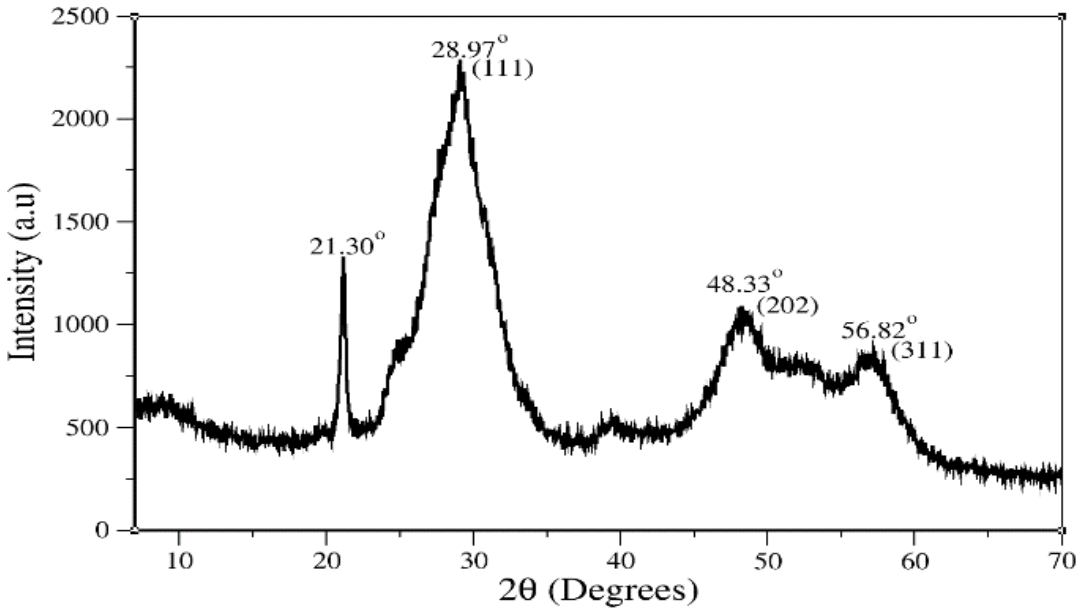

Fig. 2: XRD Pattern of ZnS nanoparticles.

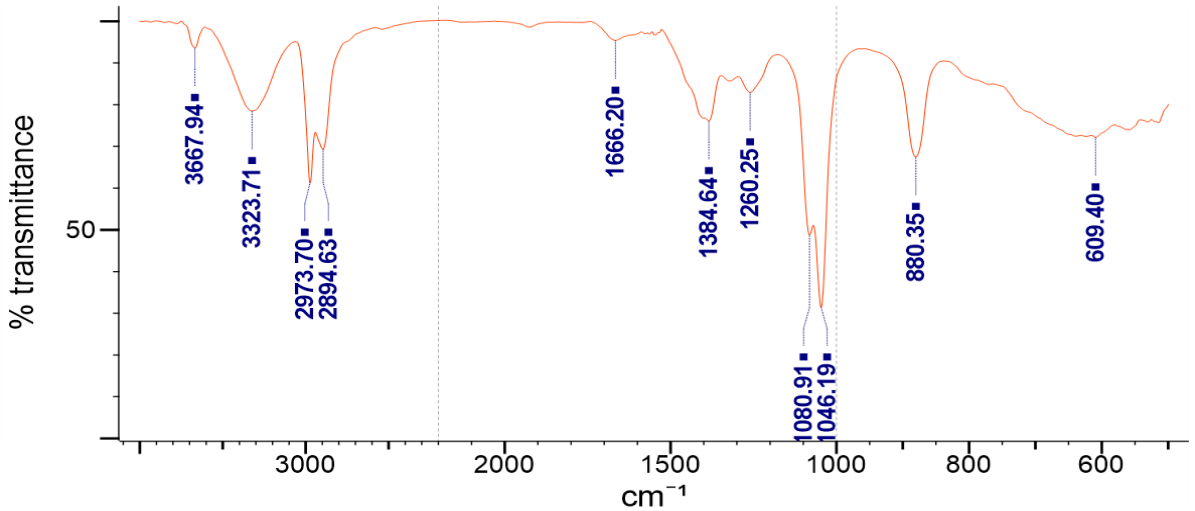

Fig. 3: Fourier transform infrared (FTIR) spectrum of ZnS.

3.2. Device Characterization

3.2.1. *Electrical Conductivity of the Counter Electrode Thin Films*

In DSSCs, the CE is essential for facilitating electron transfer and catalyzing the reduction of the redox electrolyte. The performance of the CE is strongly influenced by its electrical properties, particularly electrical conductivity. Table 1 provides the sheet resistance and electrical conductivity values of the ZnS and Pt thin films used as CEs. Between the two materials, Pt exhibited the best electrical performance, with a low sheet resistance of 190.77 Ω/sq and a higher electrical conductivity of 379.85 S/m. These values are consistent with Pt's well-known role as an excellent conductor and catalyst in DSSCs, where it facilitates efficient charge transfer at the CE-electrolyte interface (Grätzel, 2003). ZnS, on the other hand, showed a high resistance of 1331.91 Ω/sq and low conductivity of 54.41 S/m. This may stem from low carrier density, defect-related trap states, and the limited interparticle electrical connectivity. Although platinum exhibits better electrical conductivity and catalytic activity, its high cost, scarcity, and susceptibility to electrolyte corrosion significantly limit the large-scale commercial deployment of DSSCs. In contrast, ZnS nanomaterials offer a low-cost, earth-abundant, and chemically stable alternative. With proper engineering or hybridization with other inexpensive conductive materials, ZnS-based counter electrodes can provide competitive catalytic performance while dramatically reducing device fabrication costs.

Table 1: Electrical conductivity of the counter electrodes.

Counter electrode (CE) thin film	Sheet resistance, ±0.005 (Ω/sq)	Electrical conductivity ±0.005 (S/m)	Thin film thickness ±0.05 (μm)
ZnS	1331.91	54.41	3.8
Pt	190.77	379.85	1.8

3.2.2. *Photovoltaic Performance of DSSCs Utilizing ZnS Counter Electrodes*

The photovoltaic performance of DSSCs incorporating ZnS nanomaterials was investigated and compared with the reference Pt CE devices. To investigate the importance of optimal annealing of ZnS-based CE, two CEs were made. One was heat-treated at 100°C, which was referred to as ZnS-1, and one was annealed at 400 ^{0}C herein referred to as ZnS-2. Among the tested materials, the ZnS-1 CE devices exhibited the lowest performance, with an efficiency of 0.07 %, while the Pt CE device obtained a PCE of 3.2 %. The observed low efficiency (0.07 %) of the ZnS-1 CE DSSCs is primarily due to its low electrical conductivity and suboptimal catalytic activity toward the I^-/I_3^- redox couple. On annealing the CE at 400 ^{0}C, the crystalline quality of ZnS nanoparticles is enhanced by reducing lattice defects and disordered grain boundaries (Bashar et al., 2020). This structural ordering facilitates better electron mobility and minimizes charge trapping sites, leading to improved charge transfer efficiency at the CE/electrolyte interface. Additionally, annealing removes synthesis-related impurities from the ZnS surface, resulting in better particle-to-particle contact and more efficient electron transport pathways, thus improving electrical connectivity between nanoparticles (Mohammed, 2021). For these reasons ZnS-2 based CE device exhibited better performances in V_{oc}, J_{sc} and the FF whose overall effect saw the PCE improve from 0.07 % to 1.1 % as shown in Table 2 and Fig. 4. These findings demonstrate that ZnS nanomaterials, when properly optimized, engineered and potentially hybridized with other low-cost conductive materials, hold significant promise as viable alternatives to Pt for low-cost DSSC fabrication. Similar improvements resulting from annealing have been reported in other materials like sulphide-based CEs. For instance, when cobalt sulphide (CoS) based CE was annealed, high crystallinity was observed, which enhanced its electrocatalytic activity (Congiu et al., 2015). In nickel sulphide (NiS) based CEs, annealing equally improved the crystallinity of the material, but in this case, not only was catalytic activity improved, but also it corresponded to faster charge transfer, which led to enhanced photovoltaic performances (Wu et al., 2017). Overall, these findings clearly demonstrate that the performance of ZnS-based CE is highly dependent on its structural quality. Herein, annealing emerged as a simple yet powerful strategy for enhancing crystallinity,

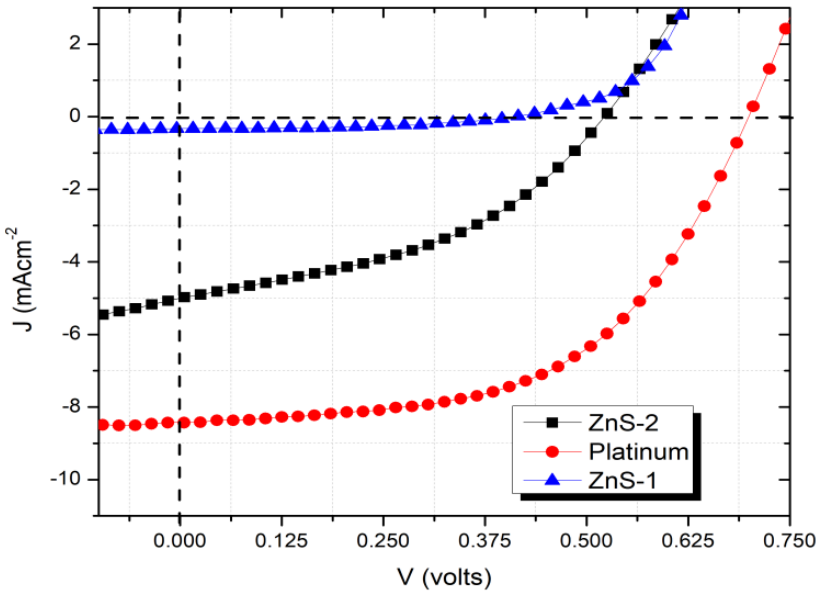

Fig. 4: The *J-V* characteristic curves of DSSCs with different CE materials.

improving charge-transfer kinetics, and suppressing recombination losses. Additionally, ZnS nanomaterials' performance confirms the unique properties in metal chalcogenides exhibiting diverse compositions, tunable molecular structures, and unique physicochemical properties, making them attractive candidates to replace noble-metal electrocatalysts in applications such as fuel cells, water electrolysis, and DSSCs. This was confirmed by Chen et al. (2010). When semitransparent FeS_2 thin films were fabricated on ITO/PEN substrates, and following surface modification, the FeS_2-based CE enabled the DSSC to achieve a power conversion efficiency of 7.31% (Wang et al., 2013). Similarly, Batabyal et al. employed $Co_{8.4}S_8$, Ni_3S_2, and $Cu_{1.8}S$ as CEs in DSSCs, achieving PCEs of 6.50%, 7.01%, and 3.79%, respectively (Mulmudi et al., 2011)

Table 2: Photovoltaic parameters of the DSSCs with ZnS-based CE.

Counter electrode Material	*Voc* (V)	*Jsc* (mAcm^{-2})	*FF* (%)	*η* (%)
ZnS-1	0.41	0.34	38.45	0.07
ZnS-2	0.52	5.02	41.97	1.10
Pt	0.69	8.43	54.36	3.21

4. Conclusion

In this study, ZnS was synthesized using a chemical reduction method and utilized in the counter electrode of DSSCs. The XRD diffraction patterns showed high crystallinity of the ZnS nanomaterials. DSSCs with the ZnS-2 modified exhibited an improved performance with a PCE of up to 1.1 % as compared to the ZnS-1 device with a PCE of 0.07 %. This improvement in photovoltaic performance originated from an enhancement in their structural order, conductivity, and catalytic efficiency. ZnS nanoparticles synthesized via a simple and cost-effective chemical reduction method therefore exhibited desirable structural and electronic properties suitable for application as a counter electrode in dye-sensitized solar cells. This study indicates that ZnS is a promising alternative to platinum with further optimization. This offers a viable pathway toward reducing both fabrication and overall production costs of DSSCs while maintaining satisfactory photovoltaic performance.

References

Ahmad, M., Rasool, K., Imran, Z., Rafiq, M. A., & Hasan, M. M. (2011). Structural and electrical properties of Zinc sulfide nanoparticles. *2011 Saudi International Electronics, Communications and Photonics Conference (SIECPC)*, 1–4. https://doi.org/10.1109/SIECPC.2011.5876907.

Aziz, A., Ali, N., Khan, A., Bilal, M., Malik, S., Ali, N., & Khan, H. (2020). Chitosan-zinc sulfide nanoparticles, characterization and their photocatalytic degradation efficiency for azo dyes. *International Journal of Biological Macromolecules*, 153, 502–512. https://doi.org/10.1016/j.ijbiomac.2020.02.310.

Bashar, M. S., Matin, R., Sultana, M., Siddika, A., Rahaman, M., Gafur, M. A., & Ahmed, F. (2020). Effect of rapid thermal annealing on structural and optical properties of ZnS thin films fabricated by RF magnetron sputtering technique. *Journal of Theoretical and Applied Physics*, 14(1), 53–63. https://doi.org/10.1007/s40094-019-00361-5.

Bokuniaeva, A. O., & Vorokh, A. S. (2019). Estimation of particle size using the Debye equation and the Scherrer formula for polyphasic TiO 2 powder. *Journal of Physics: Conference Series*, 1410(1), 012057. https://doi.org/10.1088/1742-6596/1410/1/012057.

Chen, G., Lee, M., & Wang, G. (2010). Fabrication of dye-sensitized solar cells with a 3D nanostructured electrode. *International Journal of Photoenergy*, 2010, 1–7. https://doi.org/10.1155/2010/585621.

Choudapur, V. H., Kapatkar, S. B., & Raju, A. B. (2019). Structural and Optoelectronic Properties of Zinc Sulfide Thin Films Synthesized by Co-Precipitation Method. *Acta Chemica Iasi*, 27(2), 287–302. https://doi.org/10.2478/achi-2019-0018.

Congiu, M., Albano, L. G. S., Decker, F., & Graeff, C. F. O. (2015). Single precursor route to efficient cobalt sulphide counter electrodes for dye sensitized solar

cells. Electrochimica Acta, 151, 517–524. https://doi.org/10.1016/j.electacta.2014.11.001.

Dhonde, M., Sahu, K., Das, M., Yadav, A., Ghosh, P., & Murty, V. V. S. (2022). Review—Recent Advancements in Dye-Sensitized Solar Cells; From Photoelectrode to Counter Electrode. *Journal of The Electrochemical Society*, 169(6), 066507. https://doi.org/10.1149/1945-7111/ac741f.

Ding, S., Yang, C., Yuan, J., Li, H., Yuan, X., & Li, M. (2023). An overview of the preparation and application of counter electrodes for DSSCs. *RSC Advances*, 13(18), 12309–12319. https://doi.org/10.1039/D3RA00926B.

Fang, X., Bando, Y., Liao, M., Zhai, T., Gautam, U. K., Li, L., Koide, Y., & Golberg, D. (2010). An efficient way to assemble ZnS nanobelts as ultraviolet-light sensors with enhanced photocurrent and stability. *Advanced Functional Materials*, 20(3), 500–508. https://doi.org/10.1002/adfm.200901878.

Grätzel, M. (2003). Dye-sensitized solar cells. Journal of Photochemistry and Photobiology C: *Photochemistry Reviews*, 4(2), 145–153. https://doi.org/10.1016/S1389-5567(03)00026-1.

Ibrayeva, A., Imanbekova, Z., Abibulla, U., Tashenov, Y., Baptayev, B., & Balanay, M. P. (2025). Enhancing the stability and efficiency of dye-sensitized solar cells with MIL-125 metal-organic framework as an electrolyte additive. *Scientific Reports*, 15(1), 5883. https://doi.org/10.1038/s41598-025-89913-1.

Iranmanesh, P., Saeednia, S., & Nourzpoor, M. (2015). Characterization of ZnS nanoparticles synthesized by co-precipitation method. *Chinese Physics B*, 24(4), 0461041–0461044. https://doi.org/10.1088/1674-1056/24/4/046104.

Jubeer, E. M., Manthrammel, M. A., Subha, P. A., Shkir, M., Biju, K. P., & AlFaify, S. A. (2023). Defect engineering for enhanced optical and photocatalytic properties of ZnS nanoparticles synthesized by hydrothermal method. *Scientific Reports*, 13(1), 16820. https://doi.org/10.1038/s41598-023-43735-1.

Kang, M. H., Kim, S. H., Jang, S., Lim, J. E., Chang, H., Kong, K. jeong, Myung, S., & Park, J. K. (2018). Synthesis of silver sulfide nanoparticles and their photodetector applications. *RSC Advances*, 8(50), 28447–28452. https://doi.org/10.1039/c8ra03306d.

Kharboot, L. H., Fadil, N. A., Bakar, T. A. A., Najib, A. S. M., Nordin, N. H., & Ghazali, H. (2023). A Review of Transition Metal Sulfides as Counter Electrodes for Dye-Sensitized and Quantum Dot-Sensitized Solar Cells. *Materials*, 16(7), 2881. https://doi.org/10.3390/ma16072881.

Kim, H. S., Tran, Q. N., & Park, S. J. (2017). Gold and silver core-shell nanoparticles for light absorption enhancement of organic solar cells. *2017 22nd Microoptics Conference (MOC)*, 310–311. https://doi.org/10.23919/MOC.2017.8244610.

Li, C.-T., Chang, H.-Y., Li, Y.-Y., Huang, Y.-J., Tsai, Y.-L., Vittal, R., Sheng, Y.-J., & Ho, K.-C. (2015). Electrocatalytic Zinc Composites as the Efficient Counter Electrodes of Dye-Sensitized Solar Cells: Study on the Electrochemical Performances and Density Functional Theory Calculations. *ACS Applied Materials & Interfaces*, 7(51), 28254–28263. https://doi.org/10.1021/acsami.5b07724.

Lihua, L., Xiang, Z., Xinli, L., Jinliang, H., & Volinsky C, A. A. (2018). Synthesis and Photoluminescence of Er3+ and Yb3+ Doped ZnS Nanocrystals. *Rare Metal Materials and Engineering*, 47(6), 1744–1748. https://doi.org/10.1016/S1875-5372(18)30160-7.

Mohammed, R. Y. (2021). Annealing Effect on the Structure and Optical Properties of CBD-ZnS Thin Films for Windscreen Coating. *Materials*, 14(22), 6748. https://doi.org/10.3390/ma14226748.

Mulmudi, H. K., Batabyal, S. K., Rao, M., Prabhakar, R. R., Mathews, N., Lam, Y. M., & Mhaisalkar, S. G. (2011). Solution processed transition metal sulfides: application as counter electrodes in dye sensitized solar cells (DSCs). *Physical Chemistry Chemical Physics*, 13(43), 19307. https://doi.org/10.1039/c1cp22817j.

Naeimi, H., Kiani, F., & Moradian, M. (2014). ZnS nanoparticles as an efficient and reusable heterogeneous catalyst for synthesis of 1-substituted-1H-tetrazoles under solvent-free conditions. *Journal of Nanoparticle Research*, 16(9), 2590–2598. https://doi.org/10.1007/s11051-014-2590-0.

PAWAR, R. P. (2013). Structural and Optical Properties of Chemically Synthesized ZnS Nanoparticals. *Oriental Journal Of Chemistry*, 29(03), 1139–1142. https://doi.org/10.13005/ojc/290341.

Wang, Y., Wang, D., Jiang, Y., Chen, H., Chen, C., Ho, K., Chou, H., & Chen, C. (2013). FeS 2 Nanocrystal Ink as a Catalytic Electrode for Dye-Sensitized Solar Cells. *Angewandte Chemie International Edition*, 52(26), 6694–6698. https://doi.org/10.1002/anie.201300401.

Wu, J., Lan, Z., Lin, J., Huang, M., Huang, Y., Fan, L., Luo, G., Lin, Y., Xie, Y., & Wei, Y. (2017). Counter electrodes in dye-sensitized solar cells. *Chemical Society Reviews*, 46(19), 5975–6023. https://doi.org/10.1039/C6CS00752J.